Journal of Sound and Vibration (2000) **231**(1), 99–124
doi:10.1006/jsvi.1999.2611, available online at http://www.idealibrary.com on IDEAL®

ESTIMATION OF IN-PLANE ELASTIC PARAMETERS AND STIFFENER GEOMETRY OF STIFFENED PLATES

S. CHAKRABORTY AND M. MUKHOPADHYAY

Department of Ocean Engineering & Naval Architecture, Indian Institute of Technology, Kharagpur-721 302, *India*

(*Received* 13 *May* 1999, *and in final form* 21 *August* 1999)

An investigation on stiffened plates has been conducted for the first time to determine the elastic parameters as well as the cross-sectional dimensions of rectangular stiffeners from experimental modal data and finite element predictions, using model-updating technique. The problem is formulated as a global minimization of the error function, defined by the difference in modal properties as predicted from the finite element modelling to that obtained "experimentally". The parameter estimation problem is solved using an iterative-gradient-based minimization algorithm and can start from different randomly selected set of initial parameters. The Levenberg–Marquardt algorithm has been implemented to minimize the error function. Proper bounds are realistically chosen for the selection of the initial values of the parameters. The position, physical properties and orientation of stiffeners create considerable variations in the modal properties as compared with the bare plates of similar construction. This makes each of the stiffened plate identification problem rather unique. The position of stiffeners as well as its orientation makes certain measurement points more suitable for comparing analytical and experimental mode shapes. The optimum measurement set of co-ordinates, which can be used for the purpose of identification, is thus case specific. The geometrical properties of stiffener cross-section also affect the modes. Inclusion of different sets of modes in noisy environment and the differences in the estimated parameters are studied. A few simulated examples are presented to investigate the uniqueness and convergence of results. The methodology is found to be very accurate and robust.

1. INTRODUCTION

The finite element method, though versatile, is always based upon certain simplifying assumptions, which can only be verified by physical testing, such as modal testing. Correction of the finite element models by processing dynamic test data is an active area of research for nearly three decades [1–3]. Various methods have been suggested, but it appears that none of them has been treated as generally acceptable. It also appears that the theoretical knowledge bases as well as the experimental constraints are application-specific and may differ considerably from one field to the other [4]. As such, specific case studies are

0022-460X/00/110099 + 26 $35.00/0

needed before any such technique can be applied to practical structures with any degree of confidence.

Stiffened plates are extensively used in structures where weight saving is of considerable interest yet maintaining the required stiffness [5]. Such high-performance structures, e.g., aircraft, ship panel, submersible, etc., demand accurate determination of their dynamic characteristics. These dynamic characteristics are functions of physical properties (material properties and geometry), boundary conditions and applied loading environment. For the determination of material property parameters, destructive static testing is universally accepted, as described in relevant standards. There are alternative non-destructive static testing methods for determining only the elastic parameters, but they are less accepted among the engineering community. The destructive static tests are conducted under strict specification of sample preparation and testing environment and the results are closer to the actual elastic parameters. The main drawback of the static testing is that the deformation configuration which can be attained at the time of testing can at best be of simple geometry, such as a shape having constant curvature. Structures deform at complicated configuration in the actual operating environment at higher modes. Due to the increasing use of structures in complicated high-performance environment their behavior under higher mode of deformation has become increasingly important. This can be done through dynamic testing to compute the elastic parameters when at least a considerable number of higher modes are involved. Hence, use of dynamic testing forms a better option for obtaining more accurate solution to the problem. Testing of the actual structure which need not take into account the usual manufacturing variances associated with the material properties will render the subsequent analysis more accurate.

The literature on the subject of system identification is vast [1] and no attempt will be made here to review it. The problem here is not an identification problem in the widest sense and can be described more appropriately under the headding of model updating [2]. Two closely related fields in dynamic system identification are detection of damages [3] and characterization of materials, the latter being of major interest here. The model-updating techniques differ mainly in the selection of parameters. Earlier papers such as those by Baruch and Bar Itzhack [6], Berman [7], Berman and Nagy [8] allowed any symmetric changes to the mass and stiffness matrices. Later the approach of using physical parameters was made more popular by Chen and Garba [9], Wei and Janter [10] and Wei *et al.* [11]. Unique methods have been presented for determining Young's modulus and the Poisson ratio of isotropic plates [12, 13]. The concept of experimental modal analysis has been used successfully over the decades to solve such problems [14].

Most of the previous work uses only the frequency information as, with the present state-of-the-art of instrumentation, it is difficult to measure mode shapes accurately. Messin [15] suggested a standard $\pm 0{\cdot}15\%$ error in frequency measurement for standard hammer testing, whereas the error in mode shape can be 20 times worse. However, the paper by Grediac [16] indicates that sophisticated optical methods may improve the accuracy of measured mode shapes and these advanced techniques are likely to dominate in future.

The methodology of model updating so far is mostly applied to small flat plate or beam specimens in closely controlled laboratory environment. However, it will be much more realistic to test the stiffened structure as a whole. Usually, structures are tested under free boundary conditions [17]. To apply this methodology to existing structures, all possible boundary conditions in real situation and their effect on the final estimated parameters must be ascertained. The principles developed are applied to many complicated structural forms but the application to stiffened plates/shells is non-existent.

In this paper, a non-destructive evaluation method is presented for the determination of globally averaged elastic parameters, as well as the dimensions of rectangular stiffeners of isotropic stiffened plates. It is left to the engineer's judgement to select the parameters responsible for the discrepancies between the experimental and the analytical results. The supplied values used in real application of the cross-sectional areas of stiffeners are in fact the average cross-sectional dimensions, sampled at certain places and then averaged. The sensitivity of the modal parameters with respect to these geometrical parameters are substantial in case of certain modes, thereby justifying their inclusion as updating parameters. Hence, a slight non-uniformity in cross-section may well be misinterpreted as a corresponding change in material properties, which is actually not. Thus, by including the cross-sectional dimensions as a parameter set, what is effectively obtained is a more realistic average value of cross-sectional properties of the stiffener, which refines the further analysis. In the case of stiffened plates, the changes in dimensions of the stiffener contribute substantially to the changes in modal properties at certain modes; therefore the main engineering purpose is not to ignore the stiffener geometry and consider it as variables in the minimization process along with the material constants. The use of stiffener causes considerable changes to the frequency range as well as the type of mode shapes as compared to a bare plate of the same size and mass. The effect of position, orientation and physical dimensions of stiffeners makes each of the problem case-specific and therefore needs special attention. The position as well as the orientation of stiffeners makes certain measurement points more suitable for extracting mode shape information. Particular attention is given to the study of the effect of random noise on the estimated parameters.

2. NUMERICAL SIMULATION OF EXPERIMENTAL DATA

Unlike an ideal situation in mathematical modelling, experimental results contain "true" information, which may turn out to be an obstacle to the study of a particular feature. For example, experimental modes are complex due to the presence of damping. The boundary conditions are never perfectly achieved. The data contain all types of noises—both uncorrelated and correlated to the measurements. There may be "manufacturing variances" between parts of the structure. All these factors taken together make the localization of error difficult.

Here a simple and artificial "numerical experiment" is conducted to generate data, which contains only the information sought. In this way, the one-to-one correspondence between errors and parameters is established. It is very difficult, if not impossible, to obtain the theoretical solution of practical structures, such as stiffened plates. Hence, it has been decided to use a finite element technique to generate the necessary "experimental" modal database. An eight-noded five-degrees-of-freedom (d.o.f.) per node quadratic isoparametric plate-bending element is used for modelling the plate, whereas a three-noded isoparametric beam element having five d.o.f. per node is used to model the stiffener [18, 19]. A set of "reference" parameters is realistically chosen. It is assumed that the geometry of the plate and mass density are accurately determined and do not vary from the reference solution and they are established in advance. The boundary conditions are assumed to act "perfectly". The quality of the mesh density is chosen in such a manner that the resulting modal parameters converge within the range of usual "experimental" accuracy required for successful model updating. For frequencies this is kept as 1% of the nominal value.

Although all practical structures are continuous, we assume throughout that the hypothetical real structure is discrete. Only the first few natural frequencies, along with the corresponding mode shapes, are assumed to be "measured" and sampled at certain selected co-ordinates, which "happen" to coincide with the finite element nodes of the corresponding theoretical model. This incomplete noise-free modal database is available for identification purpose, although in actual experiments the resolution of measured frequency can be increased upto a certain limit, but not without decreasing bandwidth. Thus, a realistic limit exists for the precision level that can be achieved, given the frequency range of interest.

3. SENSITIVITY ANALYSIS

A sensitivity analysis is carried out to determine the "physical" involvement of different parameters. A set of parameters is chosen first as reference; then a finite element analysis is carried out to determine the eigenfrequencies and they are used as references. Then each parameter is increased from its reference by 10% in turn and a new finite element analysis is carried out. The normalized value of increased frequency is taken as the relative sensitivity of that parameter at that particular mode.

The normalized sensitivity versus mode diagram provides a basis to decide the inclusion of a particular set of modes in the system identification algorithm. Frequency sensitivity of Young's modulus and the Poisson ratio shows a flat relationship, which means they are equally sensitive to all modes and are not shown here.

4. SELECTION OF BOUNDS

The algorithm requires initial guess of the parameters to be updated. Usually such data are available from the manufacturer. But in case it is not fully relied upon, realistic upper and lower bounds are estimated from maximum statistical variances and from nominal values given in established standards for material properties. It is assumed that the bounds are not wide apart. The algorithm starts from a randomly selected parameter set, if initial guess is not given:

$$p_i^L = p_i^*(1 - \eta), \tag{1}$$

$$p_i^U = p_i^*(1 + \eta), \tag{2}$$

where p_i^* is the nominal value of the parameter, p_i^L the lower bound of the parameter, p_i^U the upper bound of the parameter and η the deterministic design allowable.

5. FINITE ELEMENT MODELLING

The same eight-noded five-d.o.f. per node quadratic isoparametric plate-bending element is used to model the plate portion, whereas, a three-noded isoparametric beam element having five d.o.f.s per node has been chosen to model the stiffener of the stiffened plate, as is used in simulating experimental results. The element can incorporate transverse shear deformation through a first order approximation. Only rectangular stiffener is considered here. The stiffener can be oriented arbitrarily within the plate.

A simultaneous iteration algorithm has been implemented to calculate the free undamped modal properties of the structure [20].

6. GENERATION OF NOISY DATA

Noisy data sets are generated by adding random noise with known statistical properties to the noise-free reference data sets. Here uniformly distributed random noise is generated using

$$X^* = X(1 + ra), \tag{3}$$

where X^* is the noisy data (frequency or component of eigenvector), X the noise-free reference data, r the uniformly distributed sequence of random numbers between -1 and $+1$ and a the amplitude of noise.

7. FORMATION OF OBJECTIVE FUNCTIONS

The objective function consists of three terms, one relating to the error in natural frequencies E_ω, another relating to the error in mode shapes E_ϕ, and the third one for internal penalty which “explodes” at the boundary [21], E_p. These individual terms have relative weights. The total error term is

$$E = W_\omega E_\omega + W_\phi E_\phi + W_p E_p, \tag{4}$$

where W_ω is the weighting factor to the differences in natural frequencies, W_ϕ the weighting factor to the differences in mode shapes and W_p the weighting factor to the internal penalty functions.

The objective function for frequency error is just a weighted sum of the square of the differences in the natural frequencies, provided the modes are paired correctly. This is taken care of by calculating the modal assurance criteria (MAC) correlation between two pairing modes. For exactly correlated modes, the value is 1, and for uncorrelated modes, the value is 0 [14]:

$$E_{\omega} = \sum_{j=1}^{nused} W_{w_j}(\omega_{m_j} - \omega_{a_f})^2 \tag{5}$$

where W_{w_j} is the weighting factor to the jth natural frequency, and ω_{m_j} and ω_{a_j} are the jth measured and analytical natural frequencies. *nused* is the number of modes considered. $nused < M$, where M is the number of measured modes. The individual frequencies can also be weighted differently, but are kept the same here.

The mode shape error function is

$$E_{\phi} = \sum_{j=1}^{nused} W_{\phi_j}(\phi_{m_j} - \phi_{a_j})^{\mathrm{T}}(\phi_{m_j} - \phi_{a_j}), \tag{6}$$

where W_{ϕ_j} is the weight associated with the jth mode shapes, and ϕ_{m_j} and ϕ_{a_j} are the jth measured and analytical mode shapes. Only a limited number of d.o.f.s picked out from the analytical mode shapes are paired with the corresponding measured set of co-ordinates. This depends upon the sensitivity of that displacement value with respect to the parameter. Only a subset of the vertical displacements is considered here.

The measurement points which are actually used for updating depend upon the modes selected. The data set which produces low signal levels is not considered for identification as they can create numerical instability in addition to being affected very much in the presence of random error. The presence of stiffeners makes this problem complicated and specific as it depends upon the number, orientation and dimension of stiffeners.

Internal penalty is imposed indirectly by augmenting the penalty term to the objective function,

$$E_p = \sum_{j=1}^{ncons} rr(i)\left[\frac{1{\cdot}0}{boundu(i) - x(i)} + \frac{1{\cdot}0}{x(i) - boundl(i)}\right]. \tag{7}$$

Here, $x(i)$ is the parameter, $boundu(i)$ and $boundl(i)$ are the upper and lower bounds of the ith parameter respectively. The value of $rr(i)$ is reduced in subsequent iterations, as the convergence improves, *ncons* is the number of parameters having constraints.

The relative weighting factor between the frequencies and mode shapes needs very careful consideration. Not only are the mode shapes measured with less accuracy, but they are also less sensitive to the physical parameters. But in most practical situations, there may not be sufficiently available measured frequencies, and use of mode shape information is unavoidable. The relative weight magnifies the small difference in mode shapes, thus also increasing the error associated with it and this error propagates through the system identification algorithm to pollute the estimated parameters.

A frequent source of trouble is the disparity of weight between the various components of the objective function, and thereby one part may overpower the other. Here, the orders of the different parts of the objective function are generally made nearly the same to make the system identification problem well conditioned. However, whenever sufficient frequency measurements are available, they are weighted more than the eigenvectors.

8. THE MINIMIZATION ALGORITHM

The method is based on the minimization of the sum of the differences of the modal properties (i.e. eigenfrequencies and mode shapes) between the predicted values from finite element analysis and those determined "experimentally". The algorithm can use any predefined number of co-ordinates and frequencies in the order defined by the user.

Among the gradient based multivariable optimization methods available, Cauchy's steepest descent method works well when the initial point is far away from the minimum point and Newton's method works well when the initial guess is nearer [22]. Since it is not known whether the initial guess is away from the minimum or close to it, the Levenberg–Marquardt algorithm [23] is implemented for the first time to solve such type of problems, which combines both of the above features. Therefore, it is more efficient in terms of speed of convergence. The algorithm uses a non-linear least-squares solution routine for the solution of the system of equations to estimate the parameters.

The algorithm can restart automatically if stuck to a local minimum after a predefined number of iterations. Its choice of a proper step size for minimization is adaptive. Forward difference approximation is made in calculating the derivative of objective functions with respect to the parameters, but the derivatives may also be supplied externally by other efficient methods [24, 25].

The flowchart in Figure 1 describes the whole process.

9. ORGANIZATION OF STUDY

A variety of stiffened plate problems having a varying number of stiffeners have been studied [27–32].

The methodology presented is applicable in principle to any structural configuration of the plate as well as the stiffener. Material properties of the plate and stiffener are estimated simultaneously.

The procedure is repeated for both noise-free and noisy data sets. The maximum number of iterations is limited to 10. While studying the effect of random noise, 10 iterations are taken for each data set which are generated using a uniformly distributed random number generator, i.e., the parameter estimation algorithm is run 100 times for each set of selected "experimental" modal data sets. However, a typical set of convergence curves from a particular initial parameter set for each

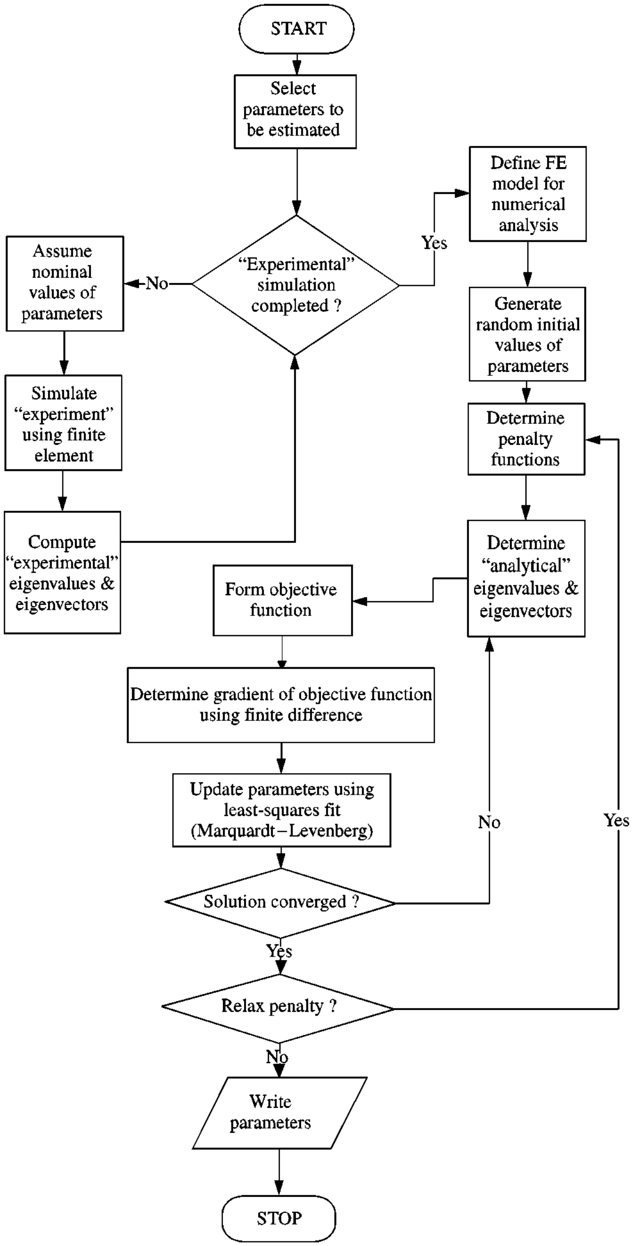

Figure 1. Flow chart of the package.

problem has been presented in the paper. The algorithm has been tested for different levels of upper and lower bounds. However, the bounds considered in the following examples are calculated putting $\eta = \pm 30\%$ in equations (1) and (2). The value of $rr(i)$ in equation (7) has been adjusted for each problem individually.

10. NUMERICAL RESULTS AND DISCUSSION

10.1. PROBLEM 1: UNIAXIALLY STIFFENED CLAMPED PLATE WITH A SINGLE STIFFENER

The geometrical and material property parameters are given in Figure 2 [27–29]. The parameters selected are the Young's modulus E, the Poisson ratio v, height of the stiffener h, and the thickness of the stiffener th. Experimental results are available in reference [27]. Details of the "measurement" points used in "numerical experiments" are given in Figure 3. The convergence of the first 12 natural frequencies are presented along with the increasing number of mesh divisions in Table 1. This investigation includes the first 7 modes; 12×12 mesh division is used. Clamped boundary conditions are assumed. Frequencies obtained are compared with standard finite element results in Table 2 and the agreement is found to be reasonably good.

As explained earlier, relevant choice of mode is essential for identification program. Observations of the mode shapes in Figure 4 and frequency sensitivity in Figure 5 indicates that the best choice of modes for identifying the height of the stiffener is 1, 2 and 7; similarly, that of identifying thickness is 1, 3 and 4. Convergence characteristics from a typical set of initial values of parameters for different mode combinations are shown in Figure 6. No significant difference in convergence is noticed for E values. The best convergence characteristics for height of the stiffener is with the mode combination 1, 4, 7. Thickness is found to converge within two iterations with the same combinations of

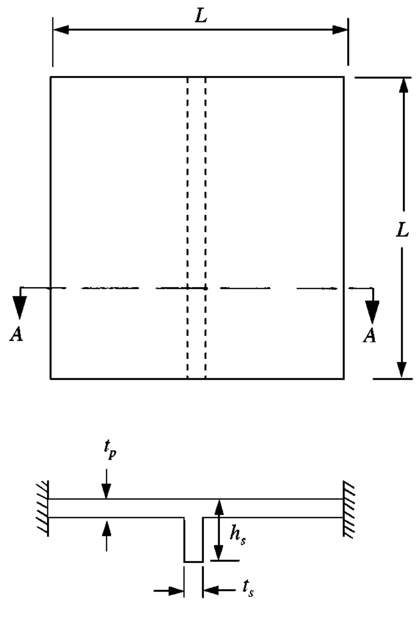

Figure 2. Uniaxially stiffened clamped plate with single stiffener: $L = 203$ mm, $t_p = 1{\cdot}37$ mm, $t_s = 6{\cdot}35$ mm, $h_s = 12{\cdot}7$ mm, $E = 68{\cdot}9$ GPa, $v = 0{\cdot}3$, $\rho = 2670$ kg/m^3.

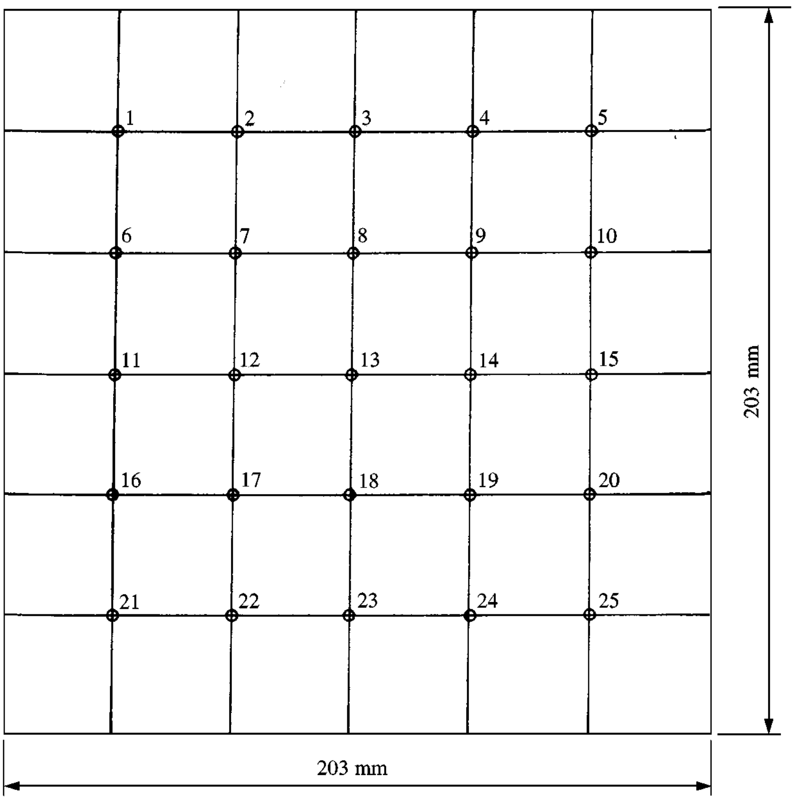

Figure 3. Measurement locations for Problems 1 and 2: ○, measurement locations.

modes. In general, the above mode combinations are found to be the best for all four parameters.

As it is necessary to estimate the effect of errors in the eigenvalues and eigenvectors on the estimated parameters, 1% random error in measured eigenvalues and 5 and 10% errors in measured eigenvectors are introduced respectively. The mean values and standard deviations are computed for at least 10 sets of noisy data and presented in Table 3. It is observed that estimated parameters are most stable for E when the first 5 modes are included. For the Poisson ratio, no considerable differences exist. This may be due to the imposition of strict internal penalty parameter $rr(i)$ as defined in equation (7) in initial stages of iterations. Height of the stiffener is best estimated when mode 7 is included. Similarly, best estimation for thickness is obtained when mode 4 is included. The convergence characteristics remain similar in the presence of random noise.

It is observed that the results are independent of the starting points in a noisy environment and depend only upon the level of noise present much in consonance with others [26]. In the no-noise cases, the parameters ultimately converge to the nominal values as shown in Figure 2. Here, the value of the objective function becomes exactly zero after minimization.

TABLE 1

Convergence of natural frequencies

	Mesh size	Mode 1	2	3	4	5	6	7	8	9	10	11	12
Problem 1 (single stiffener)	4 × 4	830·65	842·58	1173·72	1188·67	1696·32	1711·42	1930·2	4665·14	4704·37	5282·83	9506·32	11833·3
	8 × 8	744·23	780·30	1102·29	1125·17	1624·32	1662·29	1692·33	1993·41	2419·5	2463·12	2516·73	2517·20
	12 × 12	728·22	763·65	1020·06	1034·32	1466·80	1472·93	1600·49	1917·63	2100·19	2104·22	2280·79	2286·65
	16 × 16	726·72	762·24	1013·37	1027·35	1447·87	1453·23	1596·93	1906·14	2059·45	2062·38	2250·13	2256·88
	18 × 18	726·54	762·07	1012·09	1026·65	1445·91	1451·23	1596·33	1904·34	2054·88	2057·77	2246·26	2253·17
Problem 2 (cross stiffener)	4 × 4	478·39	875·37	875·37	1145·76	1378·15	1582·58	1798·02	1798·02	2794·54	4702·97	4702·97	6847·93
	8 × 8	349·31	705·82	705·82	937·66	1254·27	1303·21	1503·47	1503·47	2055·3	2055·3	2214·07	2232·09
	12 × 12	346·79	692·55	692·55	890·75	1193·32	1274·15	1385·5	1385·5	1932·97	1932·97	2000·15	2014·90
	16 × 16	346·59	691·41	691·41	887·36	1186·71	1270·80	1375·89	1375·89	1914·58	1914·58	1980·38	1990·99
	18 × 18	346·56	691·27	691·27	887·03	1185·98	1270·28	1374·85	1374·85	1912·23	1912·23	1978·05	1988·11
Problem 3 (multiple stiffener)	10 × 4	1116·43	1541·50	1541·50	1672·14	1789·08	1850·48	2111·30	2129·41	2531·90	2533·27	3219·37	4042·01
	12 × 6	1077·91	1423·40	1454·67	1619·51	1710·81	1729·96	1818·80	1842·49	2238·73	2370·91	2891·72	2948·56
	14 × 8	1081·48	1352·26	1368·46	1520·31	1603·76	1655·07	1752·55	1801·45	2150·95	2265·66	2877·98	2877·98
	16 × 10	1060·05	1291·94	1310·67	1441·77	1503·87	1537·08	1603·67	1640·71	1939·35	2160·17	2729·50	2754·02
	18 × 12	1061·85	1279·99	1296·48	1415·87	1475·23	1516·30	1576·39	1616·24	1898·08	2138·58	2662·97	2700·02

TABLE 2

Comparison of natural frequencies

		Mode number					
	References	1	2	3	4	5	6
Problem 1 (single stiffener)	Olson and Hazell [27]	718·1	751·4	997·4	1007·1	1419·8	1424·3
	Koko and Olson [28]	736·8	769·4	1019·6	1032·3	1483·7	1488·3
	Present	728·22	763·65	1020·06	1034·32	1466·80	1472·93
Problem 2 (cross stiffener)	Wu and Liu [30]	338·08	665·35	696·55	864·94	—	—
	Sheikh [31]	333·15	657·33	687·33	865·27	—	—
	Present	346·79	692·55	692·55	890·75	1193·32	1274·15
Problem 3 (multiple stiffener)	Jiang and Olson [32]	1120·7	1304·8	1312·3	1423·6	1479·4	1524·0
	Koko and Olson [28]	1112·4	1300·2	1312·2	1422·7	1479·4	1521·7
	Present	1060·05	1291·94	1310·67	1441·77	1503·87	1537·08

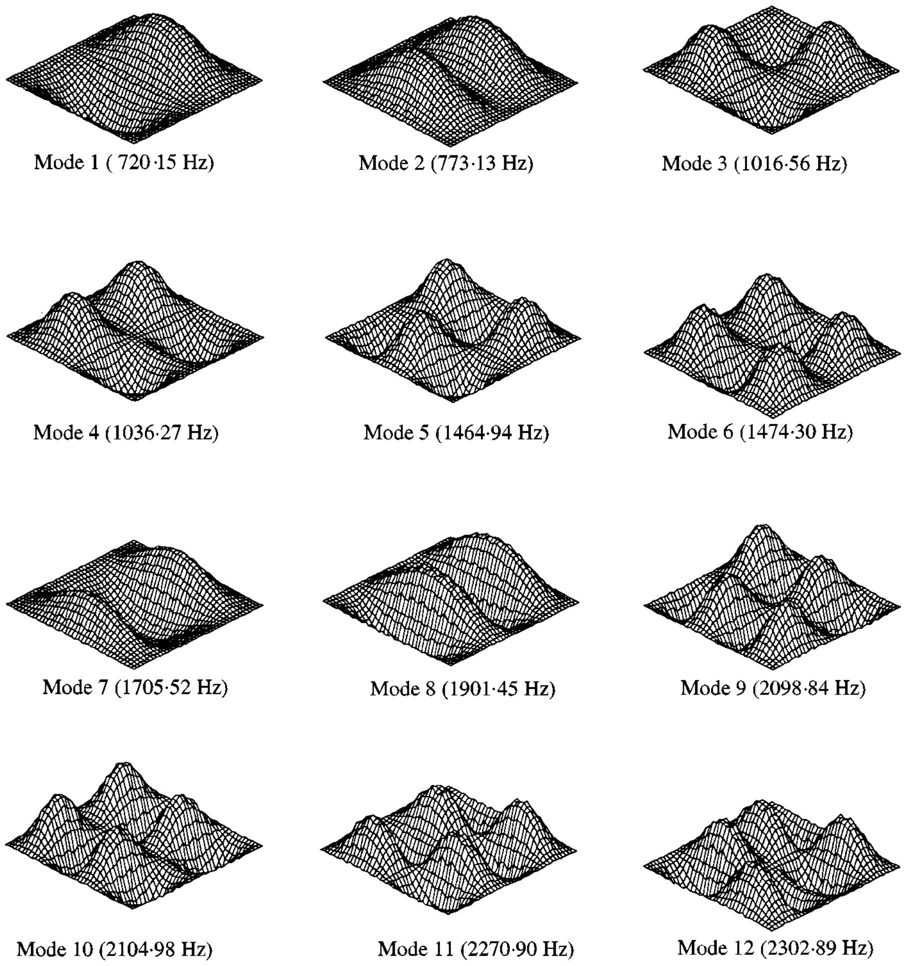

Figure 4. Mode shapes of plate with a single stiffener (Problem 1).

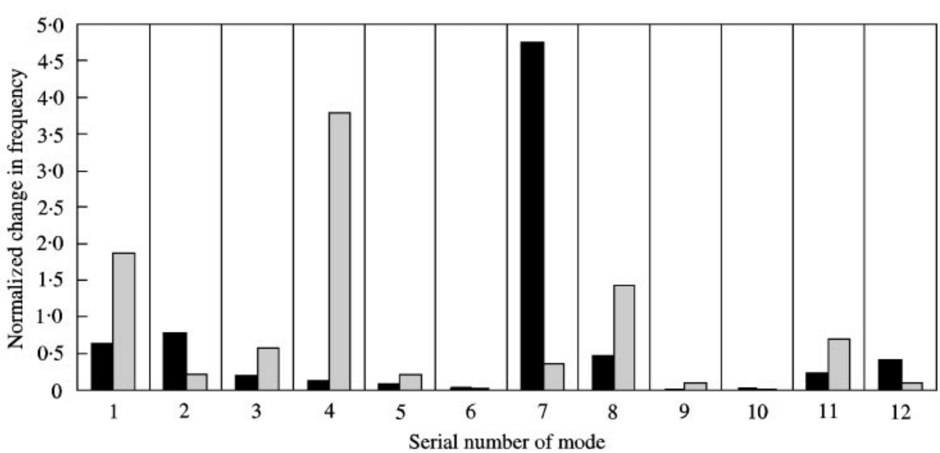

Figure 5. Frequency sensitivity diagram for Problem 1 (single stiffener): ■, height of stiffener; □, thickness of stiffener.

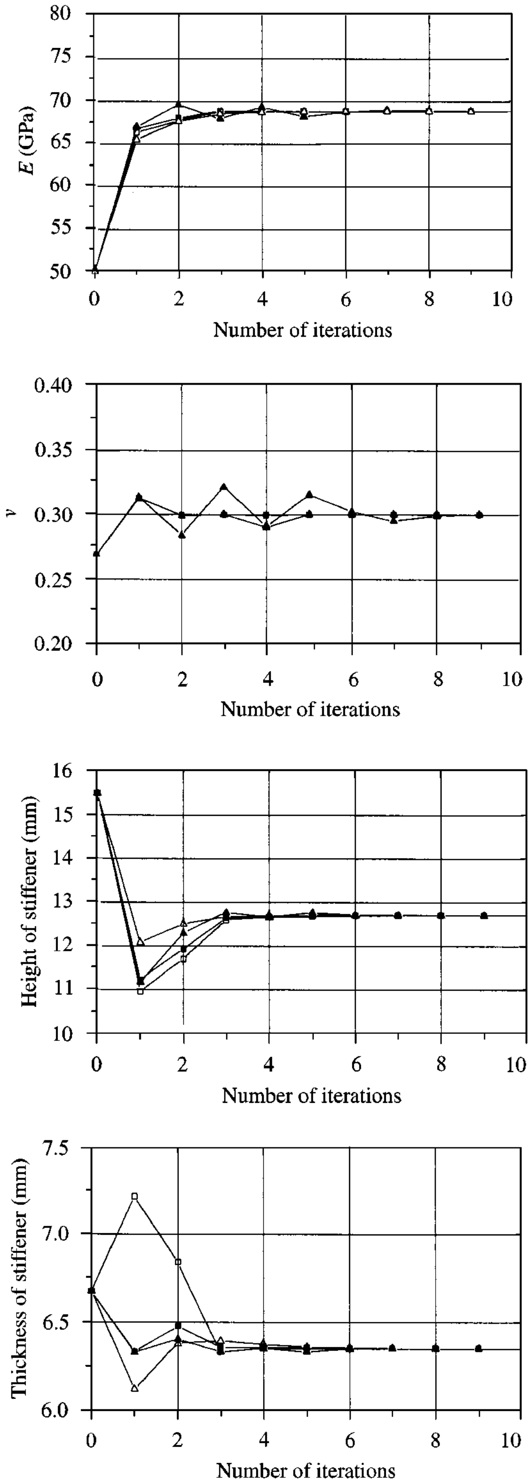

Figure 6. Convergence of parameters for Problem 1 (single stiffener): –■– modes 1–3, –□– modes 1–4, –▲– modes 1–5, –△– modes, 1, 4, 7.

TABLE 3

Influence of random errors on the identified parameters for Problem 1 (*single stiffener*)

		Selected mode combinations							
		Modes 1, 2, 3 Percentage random error		Modes 1, 2, 3, 4 Percentage random error		Modes 1, 2, 3, 4, 5 Percentage random error		Modes 1, 2, 4, 7 Percentage random error	
	Parameters	5%	10%	5%	10%	5%	10%	5%	10%
E (GPa)	Mean	68·86	69·25	68·83	68·74	68·93	69·35	68·7	68·67
	Standard deviation	0·67	1·1	0·87	1·18	0·38	0·31	0·75	0·97
	Percentage error	0·08	0·5	0·18	0·23	$<10^{-2}$	0·65	0·29	0·33
ν	Mean	0·3	0·3	0·3	0·3	0·3	0·3	0·3	0·3
	Standard deviation	0·08	0·1	0·08	0·1	0·08	0·1	0·07	0·02
	Percentage error	$<10^{-2}$	$<10^{-2}$	$<10^{-2}$	$<10^{-2}$	$<10^{-2}$	$<10^{-2}$	$<10^{-2}$	$<10^{-2}$
h (mm)	Mean	12·84	12·91	12·57	12·53	12·98	12·92	12·69	12·7
	Standard deviation	0·65	1·28	0·62	1·07	$<10^{-2}$	0·06	0·06	0·13
	Percentage error	1·11	1·71	0·96	1·36	1·73	2·2	$<10^{-2}$	$<10^{-2}$
th (mm)	Mean	6·18	6·11	6·32	6·41	6·49	6·5	6·36	6·38
	Standard deviation	0·21	0·31	0·23	0·41	$<10^{-2}$	0·01	0·22	0·42
	Percentage error	2·64	3·78	0·47	0·94	2·2	2·36	$<10^{-2}$	$<10^{-2}$

10.2. PROBLEM 2: CROSS-STIFFENED CLAMPED PLATE

The cross-stiffened plate of reference [30], [31] has been investigated. The details are given in Figure 7. Measurement locations are the same as in problem 1 and given in Figure 3. The parameters chosen for updating are the same as the previous problem. The convergence of modes with mesh divisions and comparison with references are presented in Tables 1 and 2. In fact the results shown in references [30, 31] are for elastically restrained edges; as such, the frequencies are less compared to fully clamped boundary conditions. Observations of mode shapes in Figure 8 and the frequency sensitivity diagram in Figure 9 indicate that for estimating the height of the stiffener and thickness, the best choice of modes are 1, 2, 3 and 6. Since the frequencies 2 and 3 are numerically the same, only one of these is used to avoid numerical ill-conditioning, as it happens in the case of repeated and pseudo-repeated modes.

As shown in Figure 10, the convergence is best when modes 1, 2, 5 and 6 are included. The convergence is somewhat poor when mode 6 is excluded, as expected. However, all the results have been converged properly before 10 iterations.

In the presence of noise, as shown in Table 4, E value is most stable when lower modes are involved. The height of the stiffener is best estimated with modes 1, 2, 5, 6. Thickness estimation is most stable with modes 1, 2, 6. In the absence of noise, the estimated parameters coincide exactly with the nominal values with the objective function equal to zero.

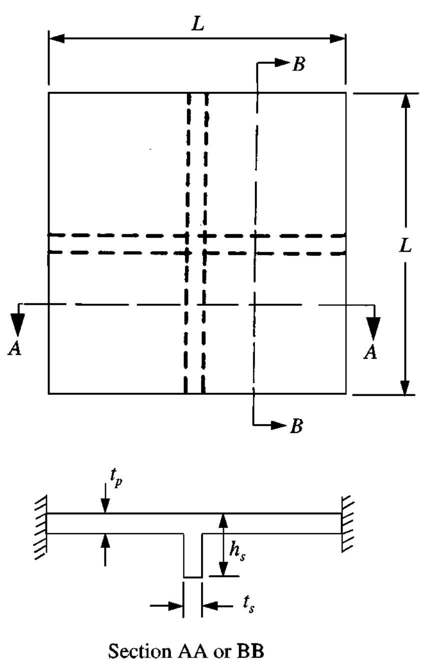

Figure 7. Cross-stiffened plate with two stiffeners: $L = 203$ mm, $t_p = 1{\cdot}37$ mm, $t_s = 2{\cdot}03$ mm, $h_s = 3{\cdot}425$ mm, $E = 68{\cdot}9$ GPa, $\nu = 0{\cdot}3$, $\rho = 2670$ kg/m^3.

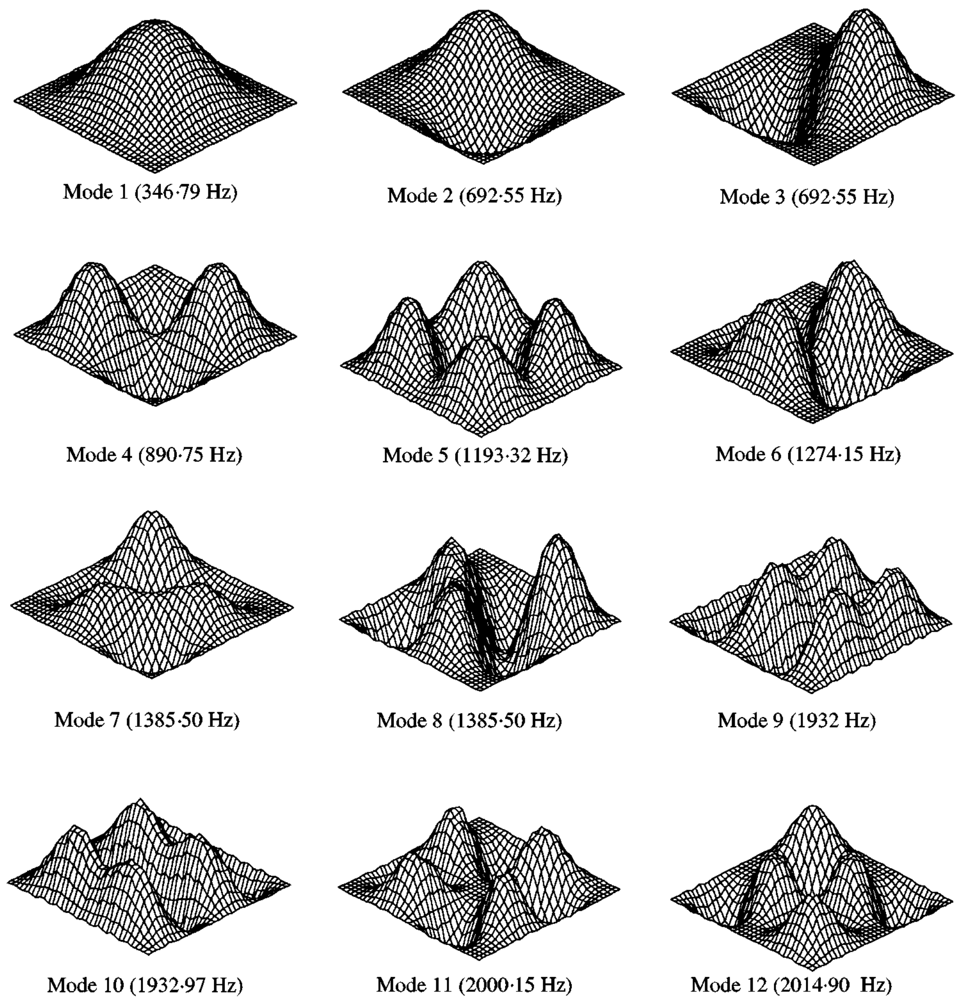

Figure 8. Mode shapes of plate with cross-stiffeners (Problem 2).

10.3. PROBLEM 3: MULTI-STIFFENED 2 × 4 BAY STIFFENED PLATE

The multi-stiffened plate of reference [32] is solved here and the details are given in Figure 11. The measurement points are shown in Figure 12. The parameters chosen for model updating are Young's modulus E, the Poisson ratio v, the height of the stiffener h, the thickness of the shorter stiffener $th1$ and the thickness of the longer stiffener $th2$. Here the number of variables are increased by one. The plate is rectangular and a mesh division of 16×10 is found to be adequate. As indicated in Tables 1 and 2, the frequencies compare well and converge properly. The mode shape diagram in Figure 13 and the frequency sensitivity diagram in Figure 14 indicate that the choice of modes for estimation of thickness is difficult as it is less sensitive.

As shown in Figure 15, mode combination 1, 2 and 3 has provided smooth convergence for all parameters, except the thickness of the longer stiffener. By

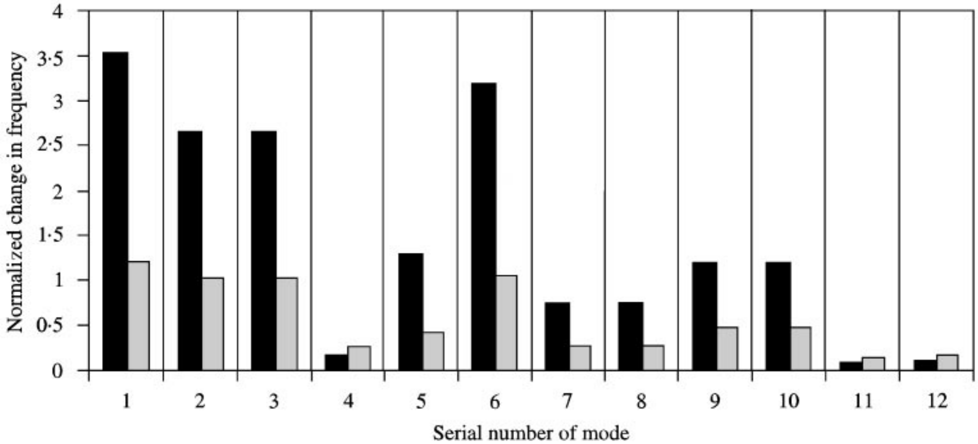

Figure 9. Frequency sensitivity diagram for Problem 2 (cross-stiffeners): ■, height of stiffener; □, thickness of stiffener.

excluding mode 1, the convergence for the height of stiffener has deteriorated. The convergence definitely improves by inclusion of all six modes, except for the thickness of longer stiffener.

In the presence of noise, as shown in Table 5, E values are estimated more accurately when lower modes are involved. By the exclusion of mode 1, the standard deviation of estimated height of the stiffener has increased. One counterintuitive result is obtained by estimating the thickness of longer stiffener. The estimated value is worst when all the 6 modes are included. This is due to the fact that the amount of error is also increased with increased information, as more and more noisy data are included.

The computer code has been written in FORTRAN77 and executed on a DEC ALPHA 1200 super minicomputer. The system time requirements to run the optimization program for a particular set of initial data and with 10 iterations were 0·5, 0·6 and 0·9 s for Problems 1, 2 and 3 respectively.

11. A BRIEF NOTE ABOUT THE REAL EXPERIMENTAL SET-UP

The set-up used for actual modal testing typically consists of an excitation mechanism, a transduction mechanism and an analyser.

The source for excitation signal can be sinusoidal, random, transient, periodic, etc. Impact excitation using hammer blow is one of the most common methods used, which produces a broadband excitation with minimum amount of equipment and set-up. To measure the force and responses, piezoelectric transducers are used extensively. Acceleration signals are measured with accelerometers, whereas the applied force is measured with force transducers. The most commonly used analyser is the spectrum analyser, where all the frequency components of the time-varying input/output complex signals are Fourier transformed and stored in a computer-like microprocessor. A suitable data-acquisition system is used to store

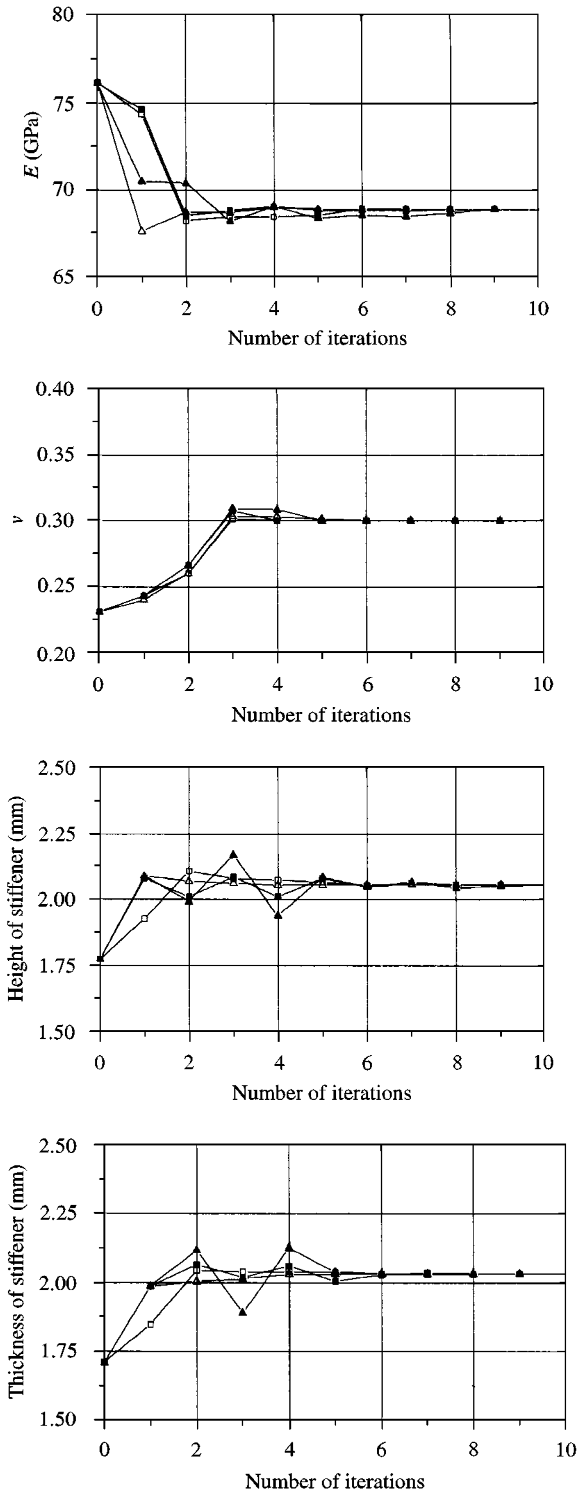

Figure 10. Convergence of parameters for Problem 2 (cross-stiffener): –■– modes 1, 2, 4, –□– modes 1, 2, 6, –▲– modes 1, 2, 4, 5, –△– modes 1, 2, 5, 6.

TABLE 4

Influence of random errors on the identified parameters for Problem 2 (cross-stiffeners)

		Selected mode combinations							
		Modes 1, 2, 4 Percentage random error		Modes 1, 2, 6 Percentage random error		Modes 1, 2, 4, 5 Percentage random error		Modes 1, 2, 5, 6 Percentage random error	
	Parameters	5%	10%	5%	10%	5%	10%	5%	10%
E (GPa)	Mean	69·21	69·57	69·02	69·09	68·55	69·26	68·85	68·29
	Standard deviation	0·66	0·59	0·36	0·71	0·4	0·8	0·46	1·00
	Percentage error	0·5	0·9	0·17	0·27	0·52	0·5	< 0·01	0·88
v	Mean	0·3	0·3	0·3	0·3	0·3	0·3	0·3	0·3
	Standard deviation	< 0·01	< 0·1	< 0·01	< 0·01	< 0·01	< 0·01	< 0·01	< 0·01
	Percentage error	—	—	—	—	—	—	—	—
h (mm)	Mean	2·00	2·01	2·056	2·055	2·054	2·061	2·051	2·06
	Standard deviation	0·016	0·014	< 0·001	< 0·001	< 0·001	< 0·001	0·016	0·017
	Percentage error	2·67	2·18	< 0·01	< 0·01	< 0·01	< 0·01	0·19	0·24
th (mm)	Mean	2·02	2·01	2·03	2·029	2·031	2·032	2·031	2·031
	Standard deviation	0·016	0·018	< 0·001	< 0·001	< 0·001	0·015	< 0·01	< 0·01
	Percentage error	0·63	1·13	< 0·01	< 0·01	0·05	0·09	—	—

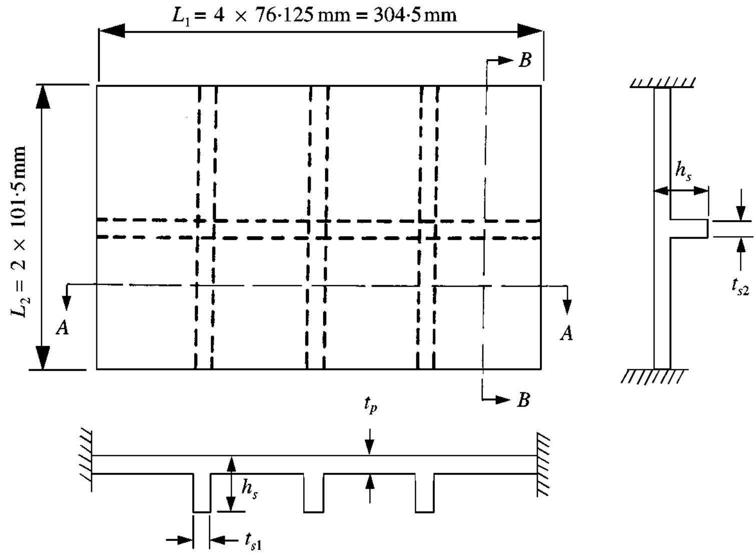

Figure 11. Multi-stiffened clamped plate with four stiffeners. $L_1 = 304{\cdot}5$ mm, $t_p = 1{\cdot}37$ mm; $t_{s2} = 6{\cdot}35$ mm, $E = 71$ GPa, $\rho = 2700$ kg/m^3, $L_2 = 203$ mm, $t_{s1} = 2{\cdot}117$ mm, $h_s = 12{\cdot}7$ mm, $\nu = 0{\cdot}3$.

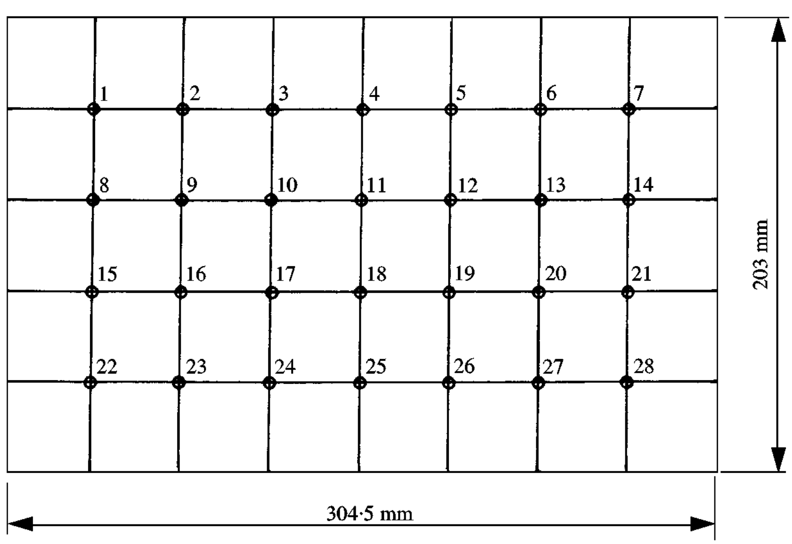

Figure 12. Measurement locations for Problem 3: ○, measurement locations.

this raw data in a PC's hard drive for further modal analysis to obtain the modal parameters.

For measuring the mode shapes using impact hammer, the response is measured at a single point whereas the excitation is applied separately at each point in turn. The measurement points which are actually used for updating, in the case of stiffened structures, depend upon the position, orientation and rigidity of stiffener.

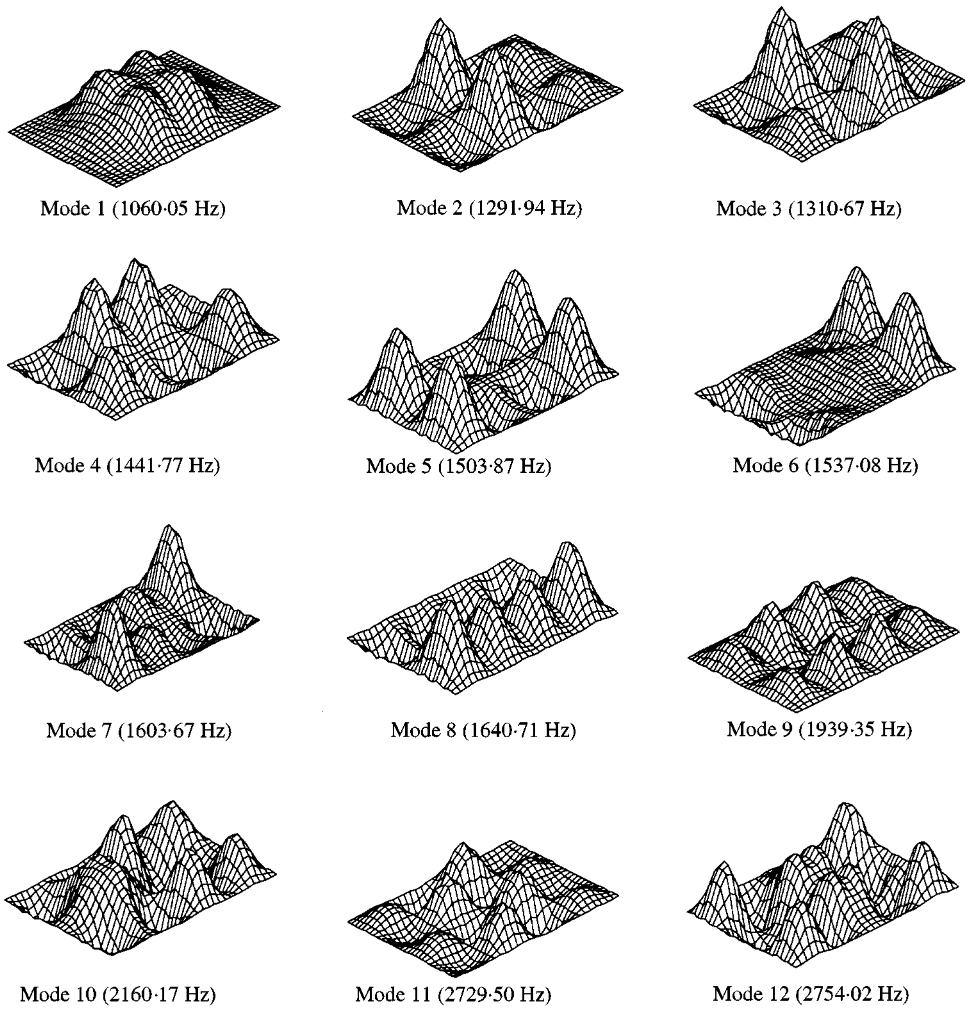

Figure 13. Mode shapes of plate with multiple stiffener (Problem 3).

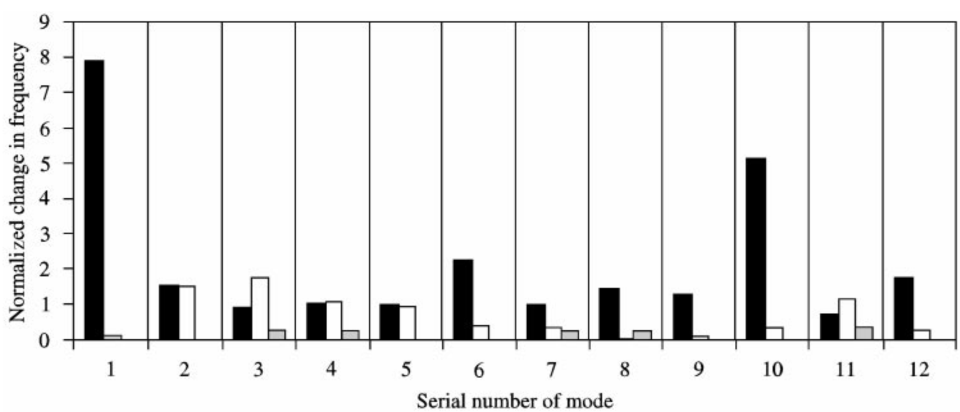

Figure 14. Frequency sensitivity diagram of Problem 3 (multi-stiffened plate). ■, height of stiffener; □, thickness of shorter stiffener; ▨, thickness of longer stiffner.

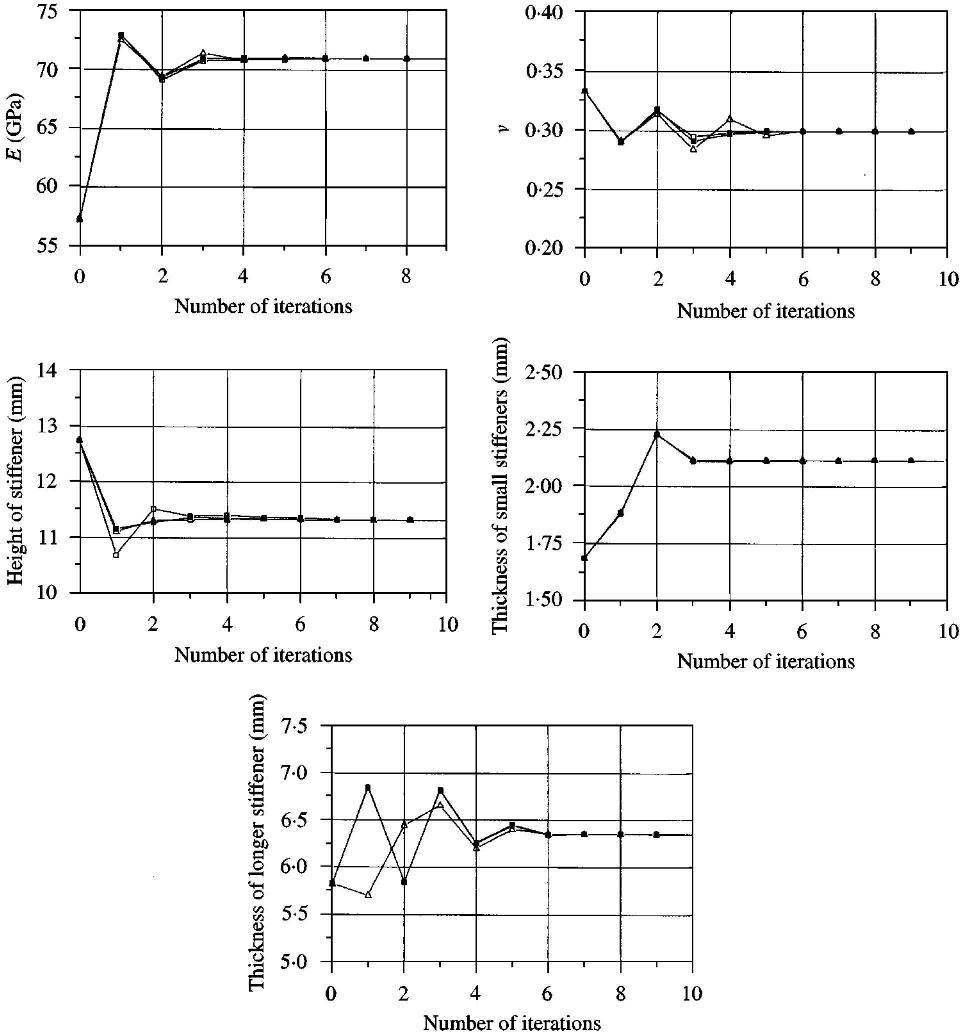

Figure 15. Convergence of parameters for Problem 3 (multiple stiffener): –■– modes 1, 2, 3, –□– modes 2, 3, 4, –△– modes 1–6.

The points which are located right over a heavy stiffener may produce very low signal level. Therefore, these points are prone to error specially in the case of noisy environment and may cause numerical instability in the updating algorithm and should be avoided.

12. CONCLUSION

An iterative method to determine the in-plane material parameters as well as the cross-sectional dimensions of rectangular stiffener of isotropic stiffened plate has been proposed in this paper. It is for the first time that a stiffened plate problem of

TABLE 5

Influence of random errors on the identified parameters for Problem 3 (multiple-stiffeners)

		Selected mode combinations					
		Modes 1, 2, 3 Percentage random error		Modes 2, 3, 4 Percentage random error		Modes 1, 2, 3, 4, 5, 6 Percentage random error	
	Parameters	5%	10%	5%	10%	5%	10%
E (GPa)	Mean	71·02	71·03	71·22	71·23	71·14	71·19
	Standard deviation	0·62	0·62	0·22	0·22	0·54	0·54
	Percentage error	0·03	0·04	0·3	0·3	0·19	0·27
ν	Mean	0·291	0·292	0·29	0·29	0·3	0·3
	Standard deviation	<0·01	<0·01	<0·01	<0·01	<0·01	<0·01
	Percentage error	—	—	—	—	—	—
h (mm)	Mean	11·32	11·32	11·32	11·31	11·32	11·31
	Standard deviation	0·07	0·07	0·09	0·09	0·07	0·08
	Percentage error	0·09	0·09	—	—	—	—
*th*1 (mm)	Mean	2·117	2·117	2·117	2·117	2·117	2·117
	Standard deviation	<0·01	<0·01	<0·01	<0·01	<0·01	<0·01
	Percentage error	—	—	—	—	—	—
*th*2 (mm)	Mean	6·345	6·345	6·345	6·345	6·24	6·23
	Standard deviation	<0·01	<0·01	<0·01	<0·01	0·45	0·50
	Percentage error	—	—	—	—	1·73	1·88

this nature has been investigated. This is also for the first time that the Levenberg–Marquardt algorithm, using non-linear least squares has been implemented for identification of parameters in plated structures. Although it is computer intensive, the methodology is found to be robust and working well even in the presence of random noise. As the method includes eigenvector information, along with frequencies, only a few modes are to be measured to estimate a number of parameters simultaneously. The method is found to be precise and stable under certain bounds over the variables, which can usually be chosen realistically from practical consideration. The proposed method may find useful application in characterizing material properties of existing stiffened structure in real environment. This is suitable for off-line mdoel updating problems where accuracy is most important. The major contribution of this paper is the estimation of material and geometric parameters simultaneously and their interaction in a spatially incomplete experimentally obtained data set. In fact, the sensitivity of the cross-sectional dimensions of the stiffeners shows that even a slight manufacturing defect in dimensions may well be misunderstood as the change in material property, which actually is not. Through the process of updating it estimates an equivalent cross-sectional dimensions which actually takes care of the variation in sectional dimensions along the length of the stiffener. It also suggests that each problem is case-specific and certain mode combinations are better than the others. Also, certain co-ordinates are best suited for measuring the mode shape depending upon the position and orientation of stiffeners, which vary from one problem to the other.

REFERENCES

1. R. BANAN and K. D. HJELMSTAD 1993 *Structural Research Serial Number* 579: *UILU-ENG*-93-2002, *University of Illinois*, *Urbana*, *IL*. Identification of structural systems from measured response.
2. J. E. MOTTERSHEAD and M. I. FRISWELL 1993 *Journal of Sound and Vibration* **167**, 347–375. Model updating in structural dynamics: a survey.
3. S. W. DOEBLING, R. F. CHARLES and B. P. MICHAEL 1998 *The Shock & Vibration Digest* **30**. A summary review of vibration-based damage identification methods.
4. S. Z. RAD and M. IMREGUN 1996 *Journal of Sound and Vibration* **196**, 323–336. On the accuracy required of experimental data for finite element model updating.
5. M. MUKHOPADHYAY and A. MUKHERJEE 1989 *Shock and Vibration Digest* **21**, 6–9. Recent advances on the dynamic behavior of stiffened plates.
6. M. BARUCH and B. ITZHACK 1978 *AIAA Journal* **16**, 346–351. Optimal weighted orthogonalisation of measured modes.
7. A. BERMAN 1979 *AIAA Journal* **17**, 1147–1148. Mass matrix correction using an incomplete set of measured models.
8. A. BERMAN and E. J. NAGY 1983 *AIAA Journal* **21**, 1168–1173. Improvement of large analytical model using modal test data.
9. J. C. CHEN and J. A. GARBA 1980 *AIAA Journal* **25**, 1494–1499. Analytical model improvement using modal test results.
10. M. L. WEI and T. JANTER 1988 *Proceedings of the* 6*th International Modal Analysis Conference*, *Kissimmee*, *FL*, 73–79. Optimization of mathematical model via selected physical parameters.
11. J. C. WEI, Q. ZHANG, R. ALLEMANG and M. L. WEI 1989 13*th International Modal Analysis Seminar*, *K. U*., *Leuven*, *Belgium*. Correction of finite element model via selected physical parameters.
12. Y. V. ZELENEV and L. M. ELECTRICA 1973 *Soviet Physics—Acoustics* **18**, 339–341. Determination of the dynamic parameters of polymer plates.
13. J. A. WOLF and T. G. CARNE 1979 *Meeting of Society for Experimental Stress Analysis*, *San Francisco*, *CA*. Identification of the elastic constants for composites using modal analysis.
14. D. J. EWINS 1984 *Modal Testing*: *Theory and Practice*. London: Research Studies Press.
15. A. MESSINA, I. A. JONES and E. J. WILLIUMS 1998 *Proceedings of the Conference on Identification in Engineering System*, *Swansea U.K*. 67–76. Damage detection and localisation using natural frequency changes.
16. M. GREDIAC *et al.* 1998 *Journal of Sound and Vibration* **210**, 643–659. Direct identification of elastic constants of anisotropic plates by modal analysis: experimental results.
17. L. R. DEOBALD and R. F. GIBSON 1988 *Journal of Sound and Vibration* **124**, 269–283. Determination of elastic constants of orthotropic plates by a modal analysis/Rayleigh–Ritz technique.
18. A. MUKHERJEE and M. MUKHOPADHYAY 1988 *Computers and Structures* **30**, 1303–1317. Finite element free vibration of eccentrically stiffened plates.
19. C. RAY 1998 *Ph.D. Thesis*, *Indian Institute of Technology*, *India*, Analysis of hat-stiffened composite plates by finite element method.

20. R. B. Corr and A. Jennings 1976 *International Journal for Numerical Methods in Engineering* **10**, 647–663. A simultaneous iteration algorithm for symmetric eigenvalue problems.
21. R. L. Fox 1971 *Optimization Methods for Engineering Design*. Reading, MA: Addison-Wesley Publishing Company.
22. K. Deb 1996 *Optimization for Engineering Design—Algorithms and Examples*. New Delhi: Prentice-Hall of India.
23. J. J. More 1977 *Numerical Analysis* Lecture Notes in Mathematics (G. A. Watson, editor), Vol. 630. Berlin: Springer-Verlag. The Levenberg-Marquardt algorithm, implementation and theory.
24. R. L. Fox and M. P. Kapoor 1968 *AIAA Journal* **6**, 2426–2429. Rates of change of eigenvalues and eigenvectors.
25. T. R. Sutter, C. J. Camada, J. L. Walsh and A. M. Howard 1988 *AIAA Journal* **33**, 1506–1511. Comparison of several methods for calculating vibration mode shape derivatives.
26. K. D. Hjelmstad 1996 *Journal of Sound and Vibration* **192**, 581–598. On the uniqueness of modal parameter estimation.
27. M. D. Olson and C. R. Hazell 1977 *Journal of Sound and Vibration* **50**, 43–61. Vibration studies on some integral rib-stiffened plates.
28. T. S. Koko and M. D. Olson 1992 *Journal of Sound and Vibration* **158**, 149–167. Vibration analysis of stiffened plates by super elements.
29. I. E. Harik and M. Guo 1993 *Journal of Computers & Structures* **49**, 1007–1015. Finite element analysis of eccentrically stiffened plates in free vibration.
30. J. R. Wu and W. H. Liu 1988 *Journal of Sound and Vibration* **123**, 103–113. Vibration of rectangular plates with edge restraints and intermediate stiffeners.
31. A. H. Sheikh 1995 *Ph.D. Thesis*, *Indian Institute of Technology*, *Kharagpur*, *India.* Linear and non-linear analysis of stiffened plate structures under static and dynamic loading by the spline finite strip method.
32. J. Jiang and M. D. Olson 1993 *International Journal for Numerical Methods in Engineering* **36**, 2219–2243. Applications of a super element model for non-linear analysis of stiffened box structures.